

See discussions, stats, and author profiles for this publication at: <https://www.researchgate.net/publication/268439657>

Analysis of climate uniformity in a naturally vented greenhouse equipped with high pressure fogging system using computational fluid dynamics

Article in *Acta horticulturae* · October 2013

DOI: 10.17660/ActaHortic.2013.1008.23

CITATIONS

2

READS

213

2 authors:



Ehab A Tamimi

University of Pittsburgh

10 PUBLICATIONS **44** CITATIONS

SEE PROFILE



Murat Kacira

The University of Arizona

77 PUBLICATIONS **945** CITATIONS

SEE PROFILE

ANALYSIS OF MICROCLIMATE UNIFORMITY IN A NATURALLY VENTED GREENHOUSE WITH A HIGH-PRESSURE FOGGING SYSTEM

E. Tamimi, M. Kacira, C. Y. Choi, L. An

ABSTRACT. *Controlled environments have long played an important role in the field of agriculture because they enable growers to more precisely regulate not only the quantity of a crop but the quality as well. Currently, most controlled environments rely on mechanical systems to regulate temperature and relative humidity within the controlled space, but these systems can be costly to install and operate. For this reason, researchers have begun investigating the efficacy of using high-pressure fogging systems and their associated control strategies in naturally ventilated greenhouses as an alternative to mechanical cooling methods. However, conducting detailed analyses of a greenhouse's aerodynamics requires carefully arrayed instruments, a consideration of many different scenarios, and a significant amount of time to compile data, not to mention the monetary cost of experimental analysis. The objective of this study, then, was to develop a 3D computational fluid dynamics (CFD) model capable of more efficiently analyzing the movement of air in a naturally ventilated greenhouse equipped with a high-pressure fogging system. The overall model included five subunits: (1) a porous media model to simulate the ways that a crop canopy will affect airflow, (2) a solar load model and (3) a discrete ordinates radiation model to simulate solar radiation, (4) a species transport and discrete phase model to simulate evaporation of droplets, and (5) an evapotranspiration (ET) model integrated with a user-defined function (UDF). The overall model predicted temperature and relative humidity within the greenhouse with percentage errors for temperature and relative humidity of 5.7% to 9.4% and 12.2% to 26.9%, respectively (given a 95% confidence interval). The average percent error between the simulated and measured ET was around 8%, and the CFD-simulated stomatal and aerodynamic resistances agreed well and were within the ranges indicated by earlier research. Having validated the overall model with experimental data, we then used a 2^d full-factorial design to determine the effects on climate uniformity produced by four factors: position of the side vent, position of the vertical sprayer nozzles, position of the horizontal sprayer nozzles, and angle of the nozzle. On the basis of our statistical analysis, we concluded that "horizontal nozzle position" was the most significant factor for climate uniformity, while the least significant factor among those evaluated was "side vent opening."*

Keywords. *CFD, Greenhouse, High-pressure fogging, Modeling, Variable-speed driver.*

Greenhouses can be mechanically ventilated and cooled by wetted-pad and fan systems, which utilize evaporative cooling to maintain the desirable greenhouse climate. However, these systems are costly and energy-intensive. Alternatively, greenhouses can be naturally ventilated, potentially in a cost-effective way that requires relatively little energy use. This latter type of ventilation is driven by the wind effect (pressure gradients across the greenhouse vents) and buoyancy effects (temperature gradients within the greenhouse). However, maintaining environmental uniformity by means of this passive cooling mechanism

remains one of the major challenges in controlled environment agriculture. Naturally ventilated greenhouses experience unpredictable environmental variations throughout, and the conditions within the greenhouse are also heavily influenced by the outside conditions. Mechanically ventilated greenhouses can also experience environmental variation between the fan and pad. Non-uniformity in the environment can lead to variations in the crop quality and characteristics. Therefore, increasing environmental uniformity throughout the greenhouse, while saving energy and water, requires robust control strategies.

High-pressure greenhouse fogging produces an evaporative cooling effect by injecting small water droplets into the greenhouse interior. As they evaporate, the droplets extract thermal energy from the surrounding environment and in so doing decrease the air temperature while increasing the relative humidity levels. Obviously, this system works best in hot, arid and semi-arid climates. However, thus far, the technology has not been widely applied even in those regions because the research needed to examine the costs of the systems and their effectiveness

Submitted for review in October 2012 as manuscript number IET 9985; approved for publication by the Information & Electrical Technologies Division of ASABE in April 2013.

The authors are **Ehab Tamimi**, Graduate Student, **Murat Kacira**, ASABE Member, Associate Professor, **Christopher Yeonsik Choi**, ASABE Member, Professor, and **Lingling An**, Assistant Professor, Department of Agricultural and Biosystems Engineering, University of Arizona, Tucson, Arizona. **Corresponding author:** Murat Kacira, 403 Shantz Building, 1177 E. 4th St., University of Arizona, Tucson, AZ 85721; phone: 520-626-4254; e-mail: mkacira@cals.arizona.edu.

at maintaining environmental uniformity has been lacking. Fogging and ventilation analysis experimentation tends to be expensive and time-consuming, and datasets tend to be restricted to measurements collected by sensors located at discrete points.

Computational fluid dynamics (CFD) has been shown to be a cost-effective tool for measuring environmental uniformity in controlled environment agriculture systems because researchers using advanced CFD modeling and the appropriate transport models can simulate and evaluate the complex phenomena that govern the environmental variables in naturally vented greenhouses equipped with fogging systems. Once validated, these models can be used to design, install, and operate high-pressure fogging systems within a specified greenhouse design and according to stipulated climates, ventilation configurations, and control strategies.

Many researchers have sought to understand the various conditions that constitute the internal climate of greenhouses. Experimental methods for quantifying environmental variables have involved tracer gases (Boulard and Braoui, 1995; Molina-Aiz et al., 2004; Bartzanas et al., 2004), advanced experimental sensors, small-scale model greenhouses (Boulard et al., 1999), and experimental wind tunnels (Kacira et al., 1998). However, experimental methods such as these have remained costly and time-consuming. In consequence, many researchers now consider computer modeling to be a viable method for determining internal climate properties. Fluid flow in controlled environments behaves according to complex equations, including those that describe the laws governing the conservation of mass, momentum, and energy, and also those that describe turbulent flow. Because scientists have been thus far unable to solve these equations analytically when dealing with complex geometries and boundary conditions, they have turned to using numerical methods. It has been shown that, given proper boundary conditions, numerical methods can be reasonably accurate at solving the equations governing such environmental variables as air velocity, temperature, and humidity. For example, Mistriotis et al. (1997) used a CFD package successfully in a study of greenhouse ventilation rates for different vent configurations. Similarly, Kacira et al. (1998), using CFD to model air exchange for a multi-span, sawtooth greenhouse, was able to show that a linear relationship existed between ventilation rate and exterior wind velocities. More recently, Bartzanas et al. (2004), in analyzing data collected using nitrous oxide as a tracer gas, relied on CFD to validate a greenhouse ventilation model. And most recently, Hong et al. (2008) used CFD to show that ventilation can be difficult to determine experimentally, and this study also indicated that a greenhouse vent can serve as both inlet and outlet at the same time. Similarly, Romero-Gomez et al. (2008, 2010), in comparing the CFD modeling results for ventilation rates to those obtained experimentally, was able to evaluate the effect of external climate conditions and insect screens on the ventilation rates of a naturally ventilated greenhouse. These studies showed that when only roof vents are kept open, high external wind speeds ($>4.5 \text{ m s}^{-1}$) are required to

provide the recommended air exchange rate of one greenhouse volume per minute.

Many early CFD modeling programs were two-dimensional because computational capacity was restricted. However, more recent CFD programs with high-speed microprocessors can model in three dimensions. This capacity has expanded the scope and accuracy of studies seeking to evaluate controlled environments. Campen and Bot (2003), for example, using a 3D CFD model to investigate the significance of wind direction, were able to conclude that wind direction is an important factor to consider when studying ventilation rates. This conclusion was subsequently confirmed by Teitel et al. (2008) and Shklyar and Arbel (2004), who also used a 3D model and discussed the limitations of 2D CFD models in predicting the effect of wind direction. Other researchers have since used 3D CFD to study the effect that greenhouse vents can have on the internal airflow patterns (Fatnassi et al., 2003; Kacira et al., 2004; Bartzanas et al., 2004; Molina-Aiz et al., 2004) of naturally vented greenhouses or the influence of the different airflow rates on greenhouse microclimate under mechanical ventilation (Sapounas et al., 2008). Because experimental studies have suggested that the airflow inside tunnel greenhouses is highly turbulent (Boulard and Wang, 2002), many researchers, to account for this phenomenon, have utilized turbulence models such as the k - ϵ model, which solves for the turbulent kinetic energy (k) and its dissipation energy (ϵ) (Mistriotis et al., 1997; Kacira et al., 2004; Bournet et al., 2007; Rohdin and Moshfegh, 2007; Kim et al., 2008). Other researchers have shown that these models are accurate at predicting turbulent behavior. Furthermore, a number of researchers have considered the effect of natural convection by applying the Boussinesq approximation, which couples the energy and momentum equations (Choi and Kim, 1996; Bartzanas et al., 2004; Majdoubi et al., 2009; Fidaros et al., 2010; Tadj et al., 2010). Others, however, in considering the effect of buoyancy to be negligible for greenhouse settings, did not take into account the buoyancy effect caused by the speed of the external wind (Lee and Short, 2000; Campen and Bot, 2003; Kacira et al., 2004). Bot (1983), Papadakis et al. (1996), and Mistriotis et al. (1997) each reported that winds stronger than 2 m s^{-1} will dominate ventilation processes, and in such cases the effect of air temperature difference can be neglected. Buoyancy-driven ventilation becomes more important when wind speeds fall below 0.5 m s^{-1} . However, when speeds are intermediate, or exceed 0.5 m s^{-1} (where $0.5 \text{ m s}^{-1} < u < 2.5 \text{ m s}^{-1}$), ventilation is driven mostly by wind effects, although buoyancy does apparently still influence ventilation to some extent (Mistriotis et al., 1997).

Because solar radiation is an important factor, many CFD models include simulation components capable of predicting the effect of solar radiation. The discrete ordinate (DO) model is one. Now widely accepted, it allows operators to solve for the effect of solar radiation and radiative exchange (Kim et al., 2008; Bournet et al., 2007; Fidaros et al., 2010). Another significant factor is crop evapotranspiration, which can affect the internal

energy profile. Calculating the amount of heat and water exchanged between the crop and the greenhouse requires knowing the size and shape of the crop zone, and although many CFD models do not include a crop zone in their geometry, a number of researchers have employed a user-defined function (UDF) to determine evapotranspiration. Also, to simulate the effect that a crop can have on the air-velocity profile, researchers have used a porous media model to predict the momentum source term created by the presence of a crop (Boulard and Wang, 2002; Fatnassi et al., 2003; Bartzanas et al., 2004; Nebbali et al., 2012).

Compared to a conventional pad and fan system, fogging can maintain a more uniform temperature and humidity distribution. For this reason, high- and low-pressure fogging is becoming a popular way to efficiently use evaporation to cool naturally ventilated greenhouses in arid and semi-arid locations (Perdigones et al., 2008). Kim et al. (2008), one of the few CFD studies to have used a discrete phase model (DPM) to track small fogging droplets, simulated the heat and water exchange occurring between the droplets and the surroundings, and also used a species transport model to simulate water mass transport throughout the computational domain. Unlike Bournet et al. (2007), who used their validated solar radiation CFD model to investigate the ventilation rates of different theoretical greenhouse configurations, Kim et al. (2008) conducted a study and did not modify the validated fogging model layout in order to investigate different fogging configurations.

Even though CFD has been found to successfully predict humidity levels inside greenhouses equipped with fogging systems, very few articles in the literature discuss using a validated CFD model to investigate the cooling effects of different fogging setups. Therefore, the primary objective of this study is to develop a validated CFD model that will help researchers and design engineers to understand the microclimate conditions of a naturally ventilated greenhouse equipped with a high-pressure fogging system. This study also seeks to evaluate the environmental uniformity of a greenhouse operating under different fogging configurations involving a side vent opening, nozzles positioned vertically, nozzles positioned horizontally, and nozzles set at an angle.

MATERIALS AND METHODS

EXPERIMENTAL SETUP

A series of computational studies were carried out, and the results were compared with the experimental data, which were collected in a single-span research greenhouse equipped with natural ventilation and a high-pressure fogging system and used to shelter a mature tomato crop. The greenhouse used in the study is located at the University of Arizona's Controlled Environment Agriculture Center in Tucson, Arizona (111° W, 32° N). The experimental measurements were carried out during July 2010, and the data from 26 July 2010 were used for the CFD model validation performed in this study. At the

time of the experiments, the greenhouse had continuous side vents and a roof vent. To acquire the interior climatic data, we used 21 shielded and aspirated air-temperature and relative-humidity sensors (HMP50, Vaisala, Woburn, Mass.); 18 of these sensors were located at heights of 1.25 and 3.0 m, respectively, above ground level, six of each on the north, center, and south vertical planes of the crop canopy zone. The remaining three sensors were placed in the greenhouse attic. To measure air velocity, three hotwire anemometers (FMA-900, Omega, Stamford, Conn.) were installed, one at each side vent and the roof vent. For additional velocity data, one 3D sonic anemometer (model 81000, R.M. Young, Traverse City, Mich.) was set up above the canopy within the greenhouse. Solar irradiation was measured using a pyrometer (CM3, Kipp & Zonen, Delft, The Netherlands). A weather station attached to the greenhouse exterior was used to measure outside climate conditions. An insect screen with an 81 × 81 mesh size was attached to both side vents, while the roof vent remained open to the environment with no insect screen. Furthermore, 72 fogging nozzles were installed along two high-pressure water lines that extended the length of the greenhouse, with 36 nozzles distributed evenly on each side (east and west). The fogging setup was controlled from a nearby shed, which contained the fogging compressor and filters and the Argus greenhouse environmental control system (White Rock, British Columbia, Canada). The dimensions of the experimental greenhouse are shown in figure 1. Additional details regarding the greenhouse, instrumentation, and sensor deployment can be accessed from Villarreal-Guerrero et al. (2012b).

MESH SPECIFICATIONS

We used the CFD package Fluent Workshop 12.1 (ANSYS, 2011) to create the virtual domain geometry of the greenhouse (fig. 1) and to discretize the domain (meshing) and solve the governing equations for the entire domain. The overall, calculated dimensions were 68 m W × 36 m H × 160 m L. The mesh was a structured-patch conforming type with a total of 1,164,163 elements, including 249,684 nodes with a minimum element size of 10 cm. The average mesh skewness was 0.24 ± 0.15. The elements within the greenhouse were minimized by an inflation layer applied near the wall. Thus, a finer mesh was enforced within the greenhouse to account for near-wall boundary-layer effects. A non-slip wall function was used in the simulations. Similar to the elements placed near the walls, an inflation layer was applied to the vent faces on the inside of the greenhouse because the vents included a porous-jump face that simulated the effect of the insect screen. The design of the inflation layer used to simulate the vent zone was determined by modifying the layer growth rate, the number of layers, and the element size until the simulated air velocity data at the vent agreed with the experimental data that had been obtained at the same coordinates. Three hotwire anemometers, one near each side vent and one near the roof vent, were used to collect the air velocity data.

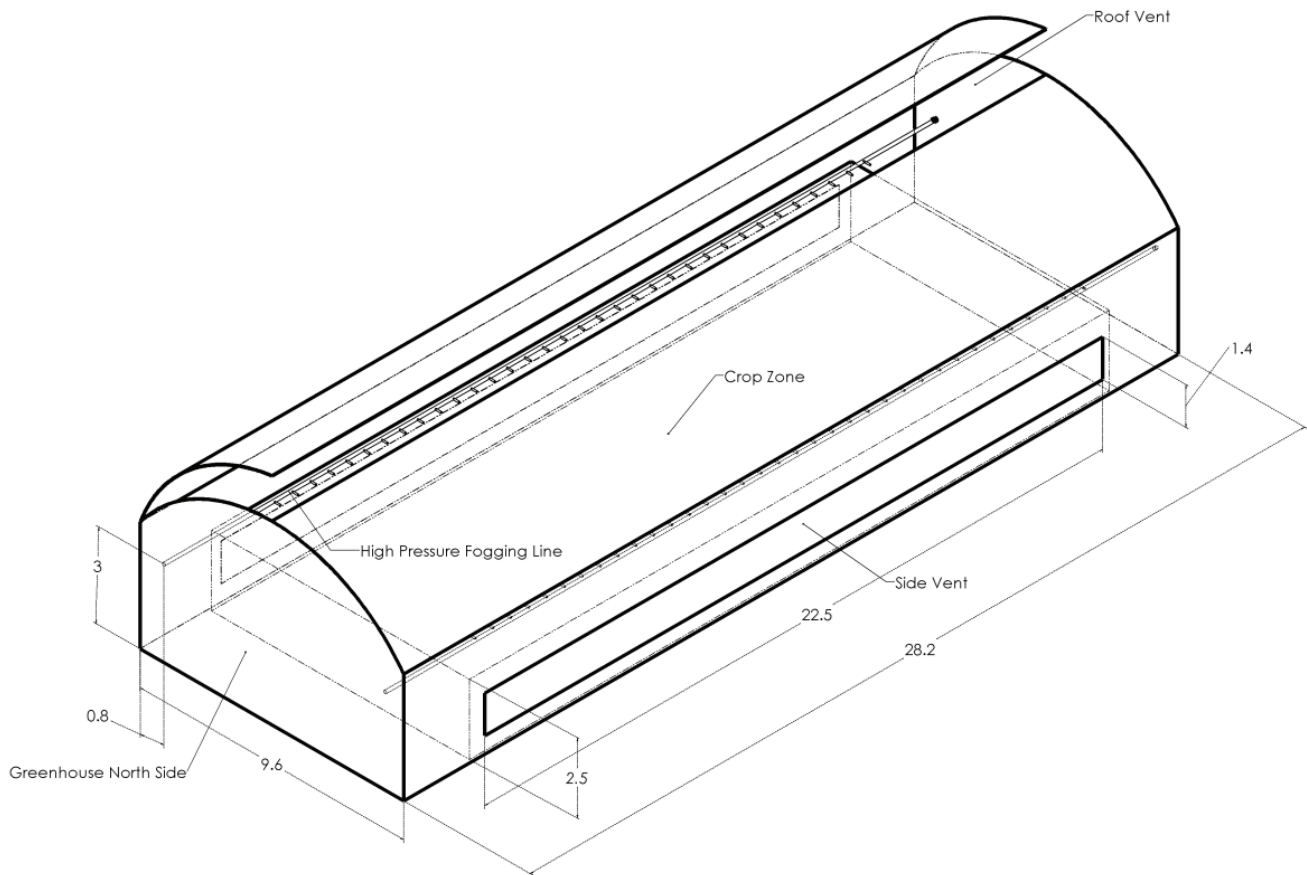


Figure 1. Diagram of the experimental greenhouse setting (all dimensions in m).

GOVERNING EQUATIONS AND BOUNDARY CONDITIONS

The CFD software package solved for the steady-state continuity, momentum, and energy equations of a three-dimensional domain in order to determine such variables as velocity, pressure, and temperature. Furthermore, to estimate humidity, the species transport model was used to determine the conservation-of-mass equation needed to calculate the water mass fraction throughout the domain. Patankar (1980) described the generalized governing equation as:

$$\frac{\partial}{\partial t}(\rho\phi) + \text{div}(\rho u\phi) = \text{div}(\Gamma \text{grad}\phi) + S \quad (1)$$

where ϕ is the variable being considered, Γ is the diffusion coefficient, and S is the source term. The simulation was performed with the assumption of steady-state conditions. Assuming the greenhouse airflow patterns to be turbulent, the standard k - ϵ turbulence model was used to solve for the turbulent kinetic energy (k) and the viscous dissipation rate of turbulent energy (ϵ). A number of researchers (Mistriotis

et al., 1997; Kacira et al., 2004; Bournet et al., 2007; Rohdin and Moshfegh, 2007; Kim et al., 2008) have shown that this model can appropriately describe the turbulent nature of fluid flow in greenhouse scenarios. The expanded, detailed version of the governing equations for mass, momentum, and energy and the k - ϵ equations can be readily found (Patankar, 1980). To realistically simulate external winds, we assigned a logarithmic wind profile equation to the wind inlet boundary conditions. We generated this equation using wind velocity data collected 2 m above the greenhouse, and we assumed a roughness length of 0.1 m (Oke, 1987). The boundary conditions of the external domain are listed in table 1.

RADIATION MODELS

Solar and Emissive Radiation Models

To simulate the effect of solar radiation flux, we used the integrated solar load model to calculate the sun position vector and integrate heat fluxes for each opaque and semi-transparent surface within the domain with respect to specific date, time, location, sky condition, solar irradi-

Table 1. Boundary conditions summary for greenhouse external domain.

Boundary	Type	Settings
West and south face	Velocity inlet	Velocity magnitude = logarithmic profile (UDF) Air temperature = 35°C; H ₂ O mass fraction = 0.0105 kg kg ⁻¹
North and east face	Pressure outlet	Backflow temperature = 35°C; backflow H ₂ O mass fraction = 0.0105 kg kg ⁻¹
Top face	Symmetry	-
Bottom face (greenhouse exterior and interior)	Wall	No slip shear condition; adiabatic diffuse opaque

Table 2. Radiative properties of greenhouse glazing material and internal ground faces.

Boundary	Type	Material	Solar Load Properties		Internal Emissivity
			Transmissivity	Absorptivity	
Side walls	Coupled wall	Polycarbonate	0.92	-	1.0
Top glazing	Couple wall	Polyethylene	0.81	-	1.0
Ground	Wall	Concrete	-	0.60	1.0

ation, and material transmissivity, absorptivity, and reflectivity. To simulate surface radiation, we used the discrete ordinates (DO) model. The DO model can solve the radiative transfer equation (RTE) for a finite number of discrete solid angles, each associated with a vector direction. Researchers have most often used the DO model to analyze controlled environmental simulation scenarios, such as the case of Bournet et al. (2007) and Kim et al. (2008). The ground surfaces of the greenhouse exterior and interior were assumed to be adiabatic and diffuse opaque surfaces in the simulations. Similar assumptions (adiabatic, diffuse, and opaque), especially with regard to the ground cover inside a greenhouse, were made by Fidasos et al. (2010) when using the DO radiation model. Furthermore, the DO model allows the solver to calculate radiation heat flux at the surface of a semi-transparent medium and has been shown to accurately simulate the behavior of greenhouse glazing. The radiative properties for all surfaces and materials used in this study are shown in table 2.

Radiation Model Validation

To validate the radiation model, a 1 m × 1 m × 1 m, simplified greenhouse prototype was constructed using polycarbonate panels similar to those used in the side walls of the experimental greenhouse. To measure air temperature, the model’s interior was equipped with a 3D matrix of eight T-type micro-thermocouples, which were connected to a data logger (model CR1000, Campbell Scientific, Logan, Utah). A pyranometer (model CM3, Kipp & Zonen, Delft, The Netherlands) was used to monitor and record solar radiation data. The experimental setup is shown in figure 2a, along with a comparison of measured and simulated data (fig. 2b). To record solar irradiation, the

mock greenhouse setup was placed outside until the inside conditions reached steady-state. A CFD model was generated for the experimental setup with appropriate boundary conditions. The simulated data compared well to the measured data, with a 2.7% to 6.2% relative error (95% confidence interval).

CROP MODEL

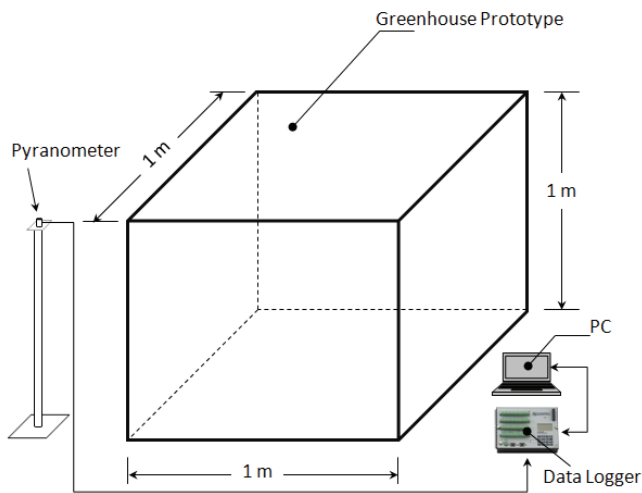
Porous Media Model

The presence of a crop inside a greenhouse affects the general airflow patterns inside the greenhouse. To account for this effect, the crop geometry can be assumed to be a porous media zone. The porous media model was only applied to the crop boundary zones, which were modeled as a rectangular block with dimensions based on experimental data (22.8 m L × 9.6 m W × 2.5 m H). The porous media model modifies equations governing the *x*, *y*, and *z* momentum by adding a velocity-dependent momentum source term (in accordance to the Darcy-Forchemier equation) to each momentum equation. The source term is calculated by the following equation:

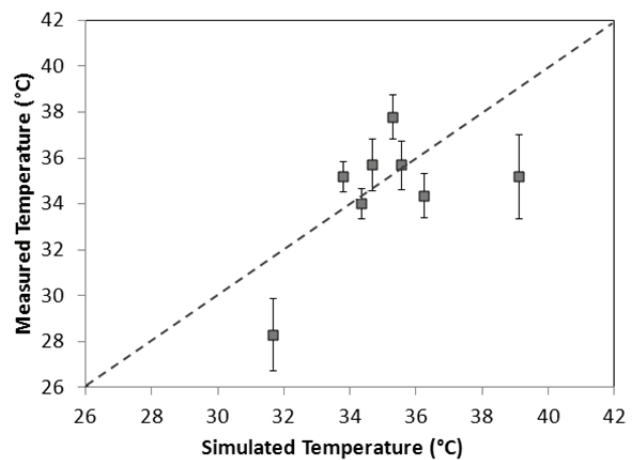
$$S = -\left(C_1\mu v + \frac{1}{2} C_2\rho v^2 \right) \tag{2}$$

where μ is the fluid viscosity ($m^2 s$), $C_1 = 1/\alpha$ is the viscous resistance (m^{-2} , where α is the permeability of the medium), C_2 is the inertial resistance factor (m^{-1}), ρ is the fluid density ($kg m^{-3}$), and v is the fluid velocity ($m s^{-1}$). The source term can also be expressed as (Sase et al., 2012):

$$S = - \rho L A D C_D v^2 \tag{3}$$



(a)



(b)

Figure 2. (a) Experimental setup for solar load model validation, and (b) comparison of measured and simulated temperature data (bars indicate standard deviations of the measured data).

where LAD is the leaf area density ($\text{m}^{-2} \text{m}^{-3}$), and C_D is the dimensionless drag coefficient. According to Sase et al. (2012), for a tomato crop in a greenhouse setting, the first term of the source term may be neglected and the equation reduced to:

$$S \approx -\frac{1}{2} C_2 \rho v^2 \quad (4)$$

Equating the coefficients from both equations results in:

$$C_2 = 2LADC_D \quad (5)$$

Sase et al. (2012) empirically calculated the dimensionless drag coefficient, $C_D = 0.31$, for a mature tomato crop in an experimental wind tunnel. Performing the appropriate calculations, $C_2 = 1.3 \text{ m}^{-1}$ for a leaf area density of $2.11 \text{ m}^2 \text{ m}^{-3}$. Furthermore, C_1 can be calculated using:

$$C_1 = \left(\frac{LADC_D}{C_f} \right)^2 \quad (6)$$

where C_f is a dimensionless non-linear momentum loss coefficient. Per the methodology presented by Sase et al. (2012), C_f is assumed to be 0.085, which results in $C_1 = 59.2 \text{ m}^{-2}$.

Porous Media Model Validation

The experimental wind tunnel setting, including a mature tomato crop, as discussed by Sase et al. (2012), was

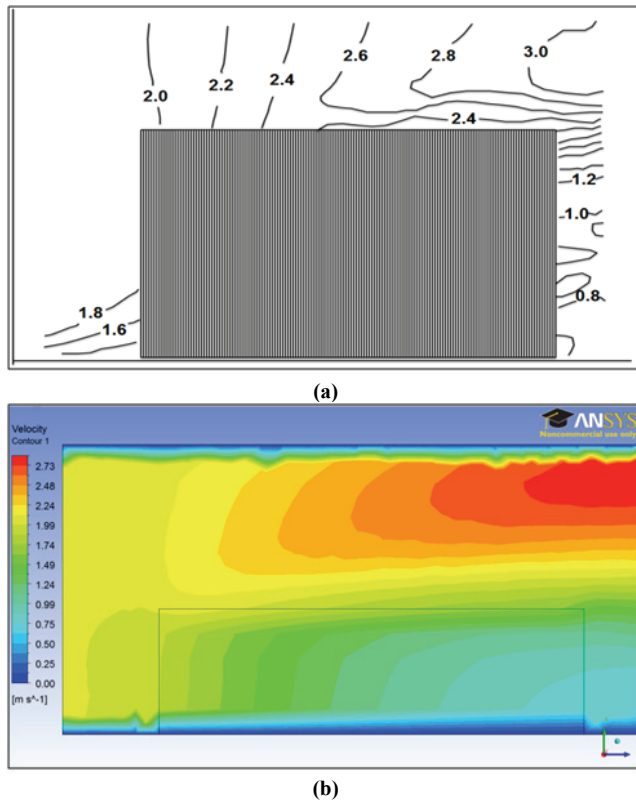


Figure 3. Porous media model validation: (a) air velocity (m s^{-1}) based on experimental data from Sase et al. (2012) and (b) simulated air velocity (m s^{-1}) using validated porous media model.

recreated using the porous media model described in the previous section. The viscous resistance and inertial resistance factor values previously calculated were used in the x , y , and z directions. The two sets of results were compared, and it was shown that the general shape of the contours was similar in both set of results (fig. 3). A notable contrast was the velocity of the air above the canopy toward the end of the air tunnel, where both measurement and simulation showed a value of around 3 m s^{-1} . Furthermore, the air velocity magnitude values in the downwind area beyond the crop were similar for both the experimental and simulated scenarios. Unlike the experimental setup, which did not measure air velocity data within the crop, the CFD model allows the user to predict the air velocity data within the crop. Overall, the comparison showed that there was a good agreement between the results obtained from the experimental data by Sase et al. (2012) and those obtained from the CFD model used in this study.

EVAPOTRANSPIRATION MODEL

Evapotranspiration (ET) from greenhouse crops is an extremely complex process because it alters the local climate, and that in turn modifies the main factors that affect ET. In addition to simulating the effect that the presence of a crop has on the airflow, it is also important to simulate the heat and water exchanged between the crop and the internal greenhouse environment. The ET process depends on a number of environmental factors, including solar radiation, humidity, air temperature, and air velocity. Since the simulation package does not include an integrated method for simulating the effect of ET, a user-defined function (UDF) was developed in order to calculate resistances, heat, and water fluxes for each cell in the crop boundary zone. The UDF is based on the energy balance as follows:

$$R_{net} = E\lambda + H \quad (7)$$

where R_{net} is the net solar irradiation at a certain crop depth (W m^{-2}), $E\lambda$ is the latent heat flux (W m^{-2}) due to ET, and H is the sensible heat flux between the crop and the environment (W m^{-2}). The net solar irradiation is a function of crop depth based on the Beer-Lambert law, adapted from Sarlikioti et al. (2011), and was calculated using the following equation:

$$R_{net} = 0.93R \cdot \exp[-0.7LAI(h_c - h)] \quad (8)$$

where R is the solar irradiation at the top of the canopy (W m^{-2}), LAI is the leaf area index ($\text{m}^2 \text{ m}^{-2}$), h_c is the height of the crop (m), and h is the vertical distance from the crop canopy top to the ground within the crop (m). To calculate the latent heat flux caused by ET within the greenhouse, the Stanghellini model was selected. It was deemed more suitable for simulating the greenhouse crop and the interior environment because it also contains the LAI term in addition to resistance terms, as shown in equation 9 (Villarreal-Guerrero et al., 2012a):

$$E\lambda = \frac{2LAI \cdot \rho C_p}{\gamma \cdot r_t} (VPD) \quad (9)$$

where C_p is the specific heat of the air ($J kg^{-1} K^{-1}$), VPD is the vapor pressure deficit on the surface of the leaf (Pa), γ is the air psychrometric constant, ($Pa \text{ } ^\circ C^{-1}$), and r_t is the total resistance ($s m^{-1}$), which can be determined by (Nebbali et al., 2012):

$$r_t = \frac{r_a^2 + Ar_s^2 + (1+A)r_s r_a}{2r_a + (1+A)r_s} \quad (10)$$

where r_a is the crop leaf aerodynamic resistance ($s m^{-1}$), r_s is the crop leaf stomatal resistance ($s m^{-1}$), and $A = \log[2.7 + (1/17)R_{net}]$. Equation 11 from Villarreal-Guerrero et al. (2012a) was used to calculate r_s , while equation 12 from Nebbali et al. (2012) was used to calculate r_a , as values calculated with this equation showed more agreement with experimental r_a measurements:

$$r_s = C_3 \frac{\frac{R_{net}}{2LAI} + C_4}{\frac{R_{net}}{2LAI} + C_5} (1 + C_6 VPD^2) \quad (11)$$

$$r_a = 305 \frac{l}{\sqrt{u + [g\beta|T_l - T_a|l\cos(\theta)]^{1/2}}} \quad (12)$$

where C_3 , C_4 , C_5 , and C_6 are constants equal to 18.6, 197.5, 0.31, and 1.2×10^{-6} , respectively, for a mature tomato crop, l is the characteristic dimension of the tomato leaf (m), g is the acceleration of gravity ($m s^{-2}$), β is the thermal expansion coefficient (K^{-1}), T_l is the leaf temperature (K), T_a is the air temperature (K), and θ is the angle between the leaf and the horizontal plane. The tomato leaf surfaces, when saturated, were assumed to be at a 0° angle and having a horizon with a 15 cm leaf characteristic dimension. The sensible heat term in the energy balance was calculated using the following equation (Nebbali et al., 2012):

$$H = 2h(T_l - T_a) \quad (13)$$

where $h = \rho C_p / r_a$ is the heat transfer coefficient ($W m^{-2} K^{-1}$). Figure 4 summarizes the process for integrating the evapotranspiration calculations into the overall simulation model. The UDF received environmental variable values from Fluent and, using the aforementioned relationships, calculated the volumetric heat and water flux values for each cell in the crop boundary zone. These values were then used as source terms for modifying the energy model and the species transport model. The calculations were performed for each iteration until the source term values converged. The accuracy of the ET model was validated in two ways: the first validation compared the CFD-simulated water flux values within the crop against experimentally measured values from Villarreal-Guerrero et al. (2012a). A sap flow rate gauge (model SGA13-WS, Dynamax, Inc., Houston, Tex.) installed at the center of the crop canopy was used to

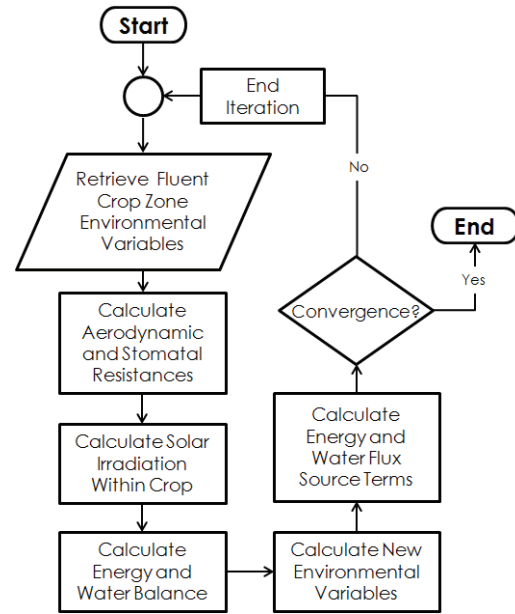


Figure 4. Flowchart of the UDF integrating evapotranspiration calculation into the overall simulation model.

measure ET rates. The average percent error that occurred between the simulated and measured ET values was around 8%. In addition, Villarreal-Guerrero et al. (2012a) measured and calculated the stomatal and aerodynamic resistances of the mature tomato crop analyzed in this study during the daytime and nighttime. The CFD-simulated stomatal and aerodynamic resistances qualitatively agreed well and were within the ranges indicated by Villarreal-Guerrero et al. (2012a). Furthermore, for post-CFD processing, the UDF also computed the relative humidity and VPD values throughout the entire domain.

DISCRETE PHASE MODEL

The discrete phase model (DPM) was used to simulate the cooling effect of the fogging (ANSYS, 2011). This model solved the equations governing multiphase flows by predicting the trajectory of a large number of particles, bubbles, or droplets of a different phase through a continuous flow field and assuming that the overall volume fraction of the second phase was relatively low. The model also predicted the exchange of energy between the continuous phase and the droplets (assumed to be around 2 microns average diameter) according to an energy balance involving sensible and latent heat transfer. The mass exchange was calculated based on the mass fraction gradient that exists between the surface of the droplet and the surrounding air. The 72 high-pressure fogging nozzles were represented in the CFD model as discrete-phase injections with fogging settings identical to the experimental setting measurements. The plain-orifice atomizer injection type was selected; this enabled the user to input nozzle specifications, such as inner diameter and length, and vapor pressure, temperature, mass flow rate, and injection direction. The model then determined the injection velocity and particle diameter distribution and calculated the effect that evaporative cooling had on the greenhouse interior. For simplification, the experimental

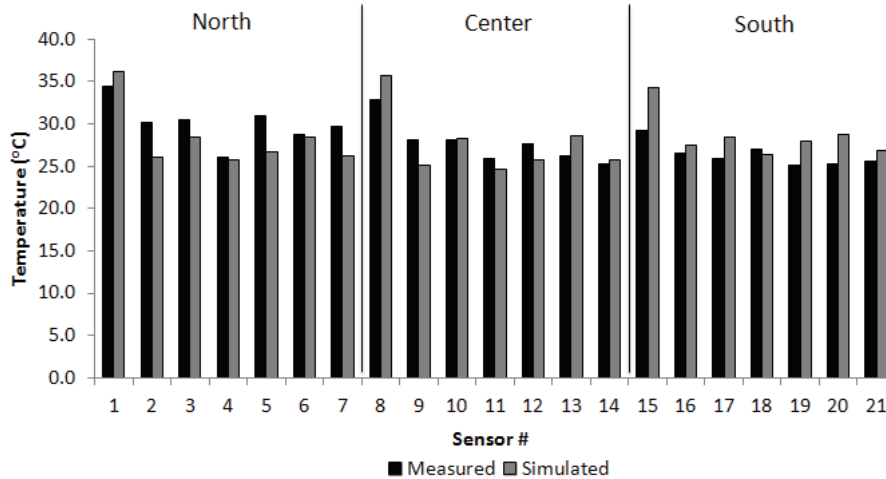


Figure 5. Comparison of measured and simulated air temperature data for 21 sensor locations in the north, center, and south sections of the experimental greenhouse.

temperature and relative humidity readings during fogging were averaged and assumed to be at steady state.

OVERALL MODEL VALIDATION

Environmental climate data were extracted from the dataset measured by Villarreal-Guerrero et al. (2012b) on 26 July 2011, when the outside air temperature was 35°C, the outside relative humidity was 35%, the outside VPD was 3.6 kPa, the wind velocity at an 8 m height was 2 m s⁻¹ at 69° from north, the outside radiation at a horizontal surface was 620 W m⁻², the fogging lines were running at a pressure of 10.3 MPa, the roof vent was 100% open, and the side vents were 100% open. This time period was chosen because the fogging system could be activated long enough to ensure that the environmental variables did not change significantly, and it could then be assumed that the conditions were at steady-state. The simulated air temperature and relative humidity at 21 points were compared to the corresponding points taken from the experimental measurements in the greenhouse interior domain, i.e., 18 points within the crop zone and three points in the attic zone, distributed evenly between the north, center, and south end of the greenhouse. The air temperature averages for the 21 location points used in the experimental and simulated datasets were 28.1°C ±2.6°C and 28.2°C ±3.3°C, respectively. The relative humidity averages for the same location points used in the experimental and simulate dataset were 73% ±17% and 82% ±18%, respectively. The measured and simulated data were compared, and a percentage error was calculated for each individual point. A percentage error of 20% and below was assumed to be good agreement. Generally, the model was more accurate in predicting the temperature and

relative humidity in the south section of the greenhouse compared to the center and north sections. The average percentage errors for temperature and relative humidity were 5.7% to 9.4% and 12.2% to 26.9%, respectively (95% confidence interval for both). Furthermore, a non-parametric Wilcoxon signed-rank statistical test was performed ($\alpha = 0.05$) in order to compare the measured and simulated data from the north, center, and south greenhouse sections separately. The resulting p-values are shown in table 3.

The statistical analysis indicated that there was a statistically significant agreement between the measured and simulated data for data points in the south section, slightly significant agreement for the center section, and less statistical agreement for the north section. This observation is confirmed by the data presented in figures 5 and 6, which show detailed comparisons between the measured and simulated air temperature and relative humidity values for the 21 location points in the three greenhouse sections. The simulated results shown in this study are based on the assumption that the outside wind profile was logarithmic and with a fix direction due to the lack of more realistic exterior wind velocity profiles, whereas in reality the wind profile could be more complicated. In addition, this study assumes steady-state conditions while using wind data from transient realistic conditions, which may have also contributed to inaccurate internal wind velocity and turbulence profiles, leading to errors between simulated and measured data. Thus, inaccuracies in wind profiles might have caused inaccurate turbulence profiles within the greenhouse, leading to overestimated relative humidity values in the center and north sections compared to the south section.

Table 3. Statistical analysis results for comparison between measured and simulated data in the north, center, and south sections in the greenhouse.

Greenhouse Section	Wilcoxon Signed-Rank Test (p-value)
North	0.0310
Center	0.0780
South	0.8125

FOGGING CONFIGURATIONS

To demonstrate the prediction capabilities of the validated model, four factors were chosen arbitrarily: the percentage at which the side vent is open, the angle at which the fogging nozzles are set, the fogging nozzles' vertical distance above the canopy, and the fogging nozzles' horizontal locations in the greenhouse. The validated model

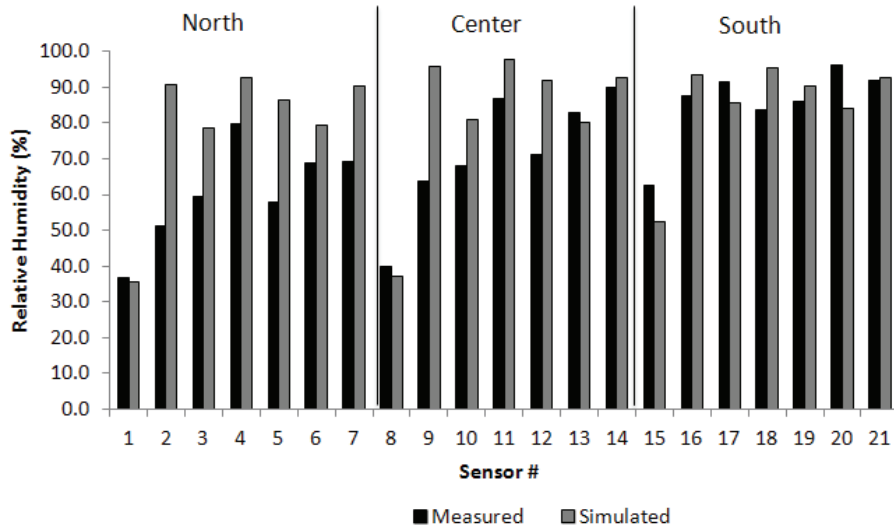


Figure 6. Comparison of measured and simulated relative humidity data for 21 sensor locations in the north, center, and south sections of the experimental greenhouse.

Table 4. Factor levels for the 2⁴ full-factorial design analysis.

Variable	Level 1	Level 2
Side vents	100%	50%
Vertical position	0.5 m	1 m
Nozzle angle	0°	45°
Horizontal position	Sides	Center

was then used to determine the effect that each factor had on the environmental uniformity of the greenhouse interior. A 2⁴ full-factorial design was created for the four factors with two levels each for statistical analysis, resulting in 16 combinations. The side vents were evaluated at 100% open (1 m) and 50% open (0.5 m), the vertical positioning of the nozzles was evaluated at heights of 0.5 and 1 m above the canopy, the nozzle angle was evaluated at 0° and 45° from the horizon, and the horizontal positioning of the nozzles was evaluated at the experimental setup along the greenhouse length and at an alternative setup along the center of the greenhouse with the 72 nozzles pointing in alternating directions and with the same nozzle properties as the original setup. The different factors and levels are summarized in table 4. Each combination was simulated using the validated model with all the necessary geometry inputted as well as all the injection property changes that corresponded with each configuration. Each scenario was solved, and the solution converged.

RESULTS AND DISCUSSIONS

COMBINATIONS DATA

The validated model was used to generate climate data for 16 combinations in order to determine if and how much each factor affected the uniformity of the greenhouse interior climate. To do this, the UDF calculated the vapor pressure deficit (VPD), which is dependent on both air temperature and relative humidity, for each node in the computational domain. Average and standard deviations were calculated based on a representative, 10,000-point random cloud collected from the greenhouse region below the gutter at a 4 m height for each combination scenario.

Table 5. Greenhouse VPD average and standard deviation values for all 16 combinations of the full-factorial design using the validated CFD model (“-” = indicates level 1, and “+” indicates level 2).

Combination	Side Vent	Vertical Position	Nozzle Angle	Horizontal Position	VPD (kPa)
1	-	-	-	-	1.25 ±0.94
2	+	-	-	-	1.12 ±0.94
3	-	+	-	-	1.15 ±0.89
4	+	+	-	-	1.14 ±0.91
5	-	-	+	-	1.35 ±0.96
6	+	-	+	-	1.38 ±0.98
7	-	+	+	-	1.44 ±0.95
8	+	+	+	-	1.28 ±0.99
9	-	-	-	+	1.99 ±1.16
10	+	-	-	+	1.83 ±1.16
11	-	+	-	+	1.68 ±1.10
12	+	+	-	+	1.67 ±1.09
13	-	-	+	+	2.38 ±1.20
14	+	-	+	+	2.24 ±1.20
15	-	+	+	+	2.31 ±1.16
16	+	+	+	+	2.13 ±1.17

The values for all 16 combinations were calculated and are shown in the table 5.

The results showed that the scenarios involving the nozzles positioned horizontally (combinations 9 through 16) generally have higher averages and standard deviations for VPD values (table 6). The VPD averages ranged between 1.12 and 2.38 kPa, while the VPD standard deviations ranged between 0.89 and 1.20 kPa throughout all the scenarios. In this study, the VPD standard deviation was used as one of the indicator of climate uniformity within the greenhouse. In addition, cross-sectional VPD contour diagrams were generated for each scenario along the center of the greenhouse’s length and width for discussions. The data indicated that the center nozzle line placement resulted

Table 6. Summary of p-values for the four factors in this study.

Factor	VPD Average (p-value)	VPD Standard Deviation (p-value)
Side vent opening	0.041	0.032
Vertical position	0.044	6.94E ⁻⁵
Nozzle angle	2.00E ⁻³	1.01E ⁻⁵
Horizontal position	3.48E ⁻⁶	8.64E ⁻⁹

in increased VPD values in the greenhouse domain compared to those values obtained when the nozzle lines were placed along the sides. The reason for this might be the fact that drier and hotter air was able to penetrate farther into the greenhouse from the vents with this configuration. It was observed that reduced side vent opening, with 0° nozzle angle and nozzle placement closer to the canopy zone, provided lower VPD values. However, in commercial operations, attention must be paid to potential effects of canopy wetting if the nozzle lines are positioned closer to the crop canopy.

Figure 7 illustrates the effect of side openings, vertical position, and nozzle angle while the fogging nozzles were in their horizontal positions on the greenhouse sides. The humidifying effects of the fogging can be seen in the cross-section of the greenhouse for each scenario, as shown by the two distinct blue areas of low VPD values. Combination 1 presents the default scenario used to validate the model. Combination 2 shows a cooling and humidification pattern similar to that of combination 1; however, lower VPD values resulted from the fact that smaller side vent openings were used, minimizing the amount of hot, dry air entering the greenhouse from the side vents. Combination 3 and 4 show the effect of vertical nozzle position; the lower VPD regions have expanded

slightly beyond the gutter line and up to the attic zone, producing an effect that was expected to occur when the nozzles were raised to a greater height. Combinations 5 through 8 show the effect of nozzle angle. Similar to the effect produced by vertical nozzle position, nozzle angle affected the expansion of the lower VPD zone beyond the gutter more toward the attic zone. However, the zone close to the ground appears to have experienced drier conditions compared to combinations 1 through 5, as the high-humidity, low-VPD zones appear to have shifted upward. The greenhouse lengthwise cross-sections show that when the side vents were 50% open, a higher concentration of humidity resulted. The greenhouse lengthwise cross-sectional diagrams for combinations 1 through 8 mostly show a concentration of low VPD values in the south end of the greenhouse, mostly likely caused by the turbulence effect produced by the angled external wind.

Figure 8 shows the VPD contours for combinations 9 through 16, evaluating the effect of side openings, vertical position, and nozzle angle when the nozzles were positioned horizontally in the center. Under the central nozzle line configuration, the effects of the evaluated factors on the greenhouse climate uniformity were different compared to those obtained from combinations 1 through 8. Instead, combinations 9 through 12 all show a similar

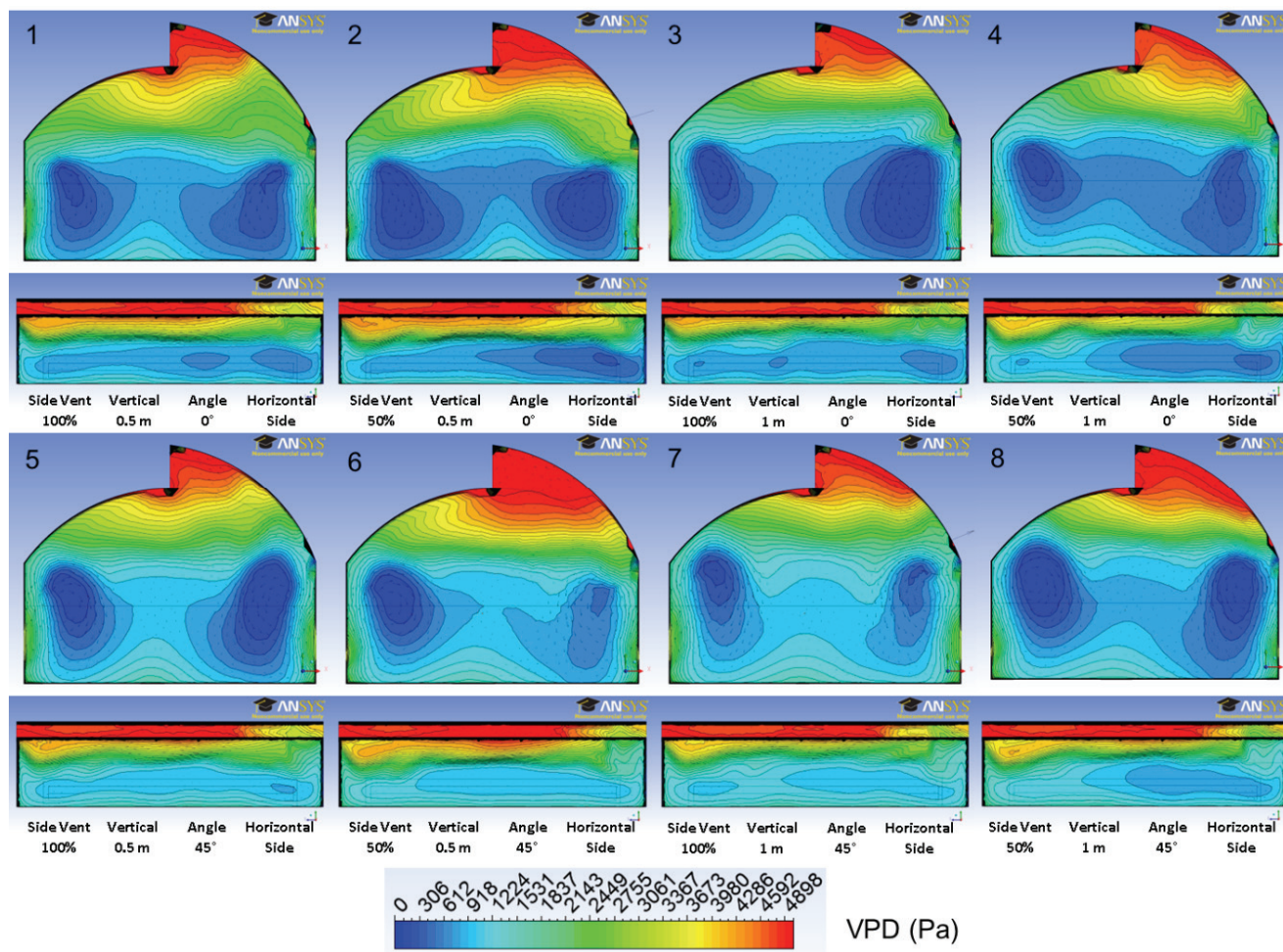


Figure 7. VPD contour diagrams for center cross-sections along the length and width of the greenhouse domain for combinations 1 through 8.

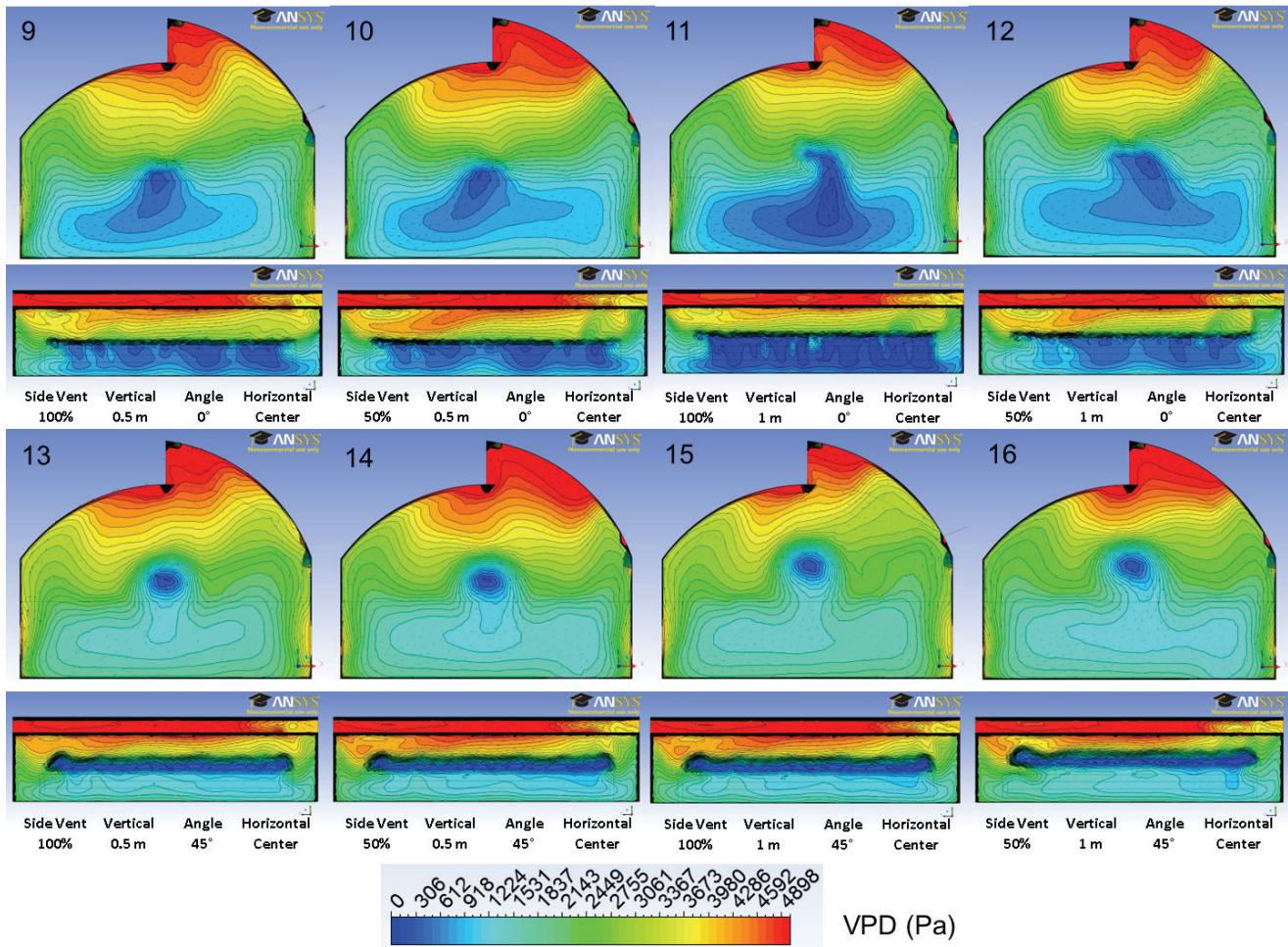


Figure 8. VPD contour diagrams for center cross-sections along the length and width of the greenhouse domain for combinations 9 through 16.

concentration of humid air in the center of the widthwise cross-section, with a humid zone mostly confined to the region below the gutter. The lengthwise cross-sections for these combinations also reveal a similar distribution of humidity along the length of the greenhouse. The effect of 0° nozzle angles providing more cooling and humidification in the zone below the gutter is clearer. Combinations 13 to 16 show the significant effect that nozzle angle had in changing the internal behavior by creating a more uniform environment for these configurations but with a higher VPD average across the greenhouse's width and along its length in the area below the gutter. An overview of combinations 9 through 16 shows that the effects of vertical position and side vent opening were minor, compared to the other factors evaluated in this study, in influencing the general airflow patterns. Unlike the diagrams for combinations 1 through 8, the lengthwise cross-sectional diagrams for combinations 9 through 16 do not show a concentration of low VPD values. Compared to the combinations that involved a side horizontal nozzle position, the VPD values for combinations 9 through 16 were relatively high in the canopy zone, in some cases above the desired threshold, for instance, for a tomato crop. All the scenarios show a circulation of the air caused by colder air falling in the

center, while warm and less dense air near the greenhouse walls rose, driven by the fogging nozzle injections. Furthermore, it should be noted that all combinations experienced relatively high VPD values near the roof vent (around 4.5 to 5.0 kPa) compared to the outside VPD value of 3.6 kPa. The size of this region varied with each combination.

Relative standard deviation (RSD) was also used (Dodge, 2003) to evaluate climate uniformity based on the VPD distribution. The RSD, sometimes also called the coefficient of variation represented as a percentage, is a measurement of the homogeneity of observations and is widely used in analytical chemistry, engineering, and physics. Compared to the usual standard deviation analysis, the RSD allows different measurements to be compared more meaningfully. Using the 10,000 cloud points mentioned earlier, the RSD values of each of the 16 combinations were calculated as $RSD (\%) = \sigma/\mu \times 100$, where σ is the standard deviation, and μ is the mean. Figure 9 presents a plot of the RSD values for the two combinations (combinations 7 and 15) that provided the lowest RSD values with more climate uniformity (of combinations 1 to 8 and combinations 9 to 16, respectively). The lower the RSD value, the more uniform

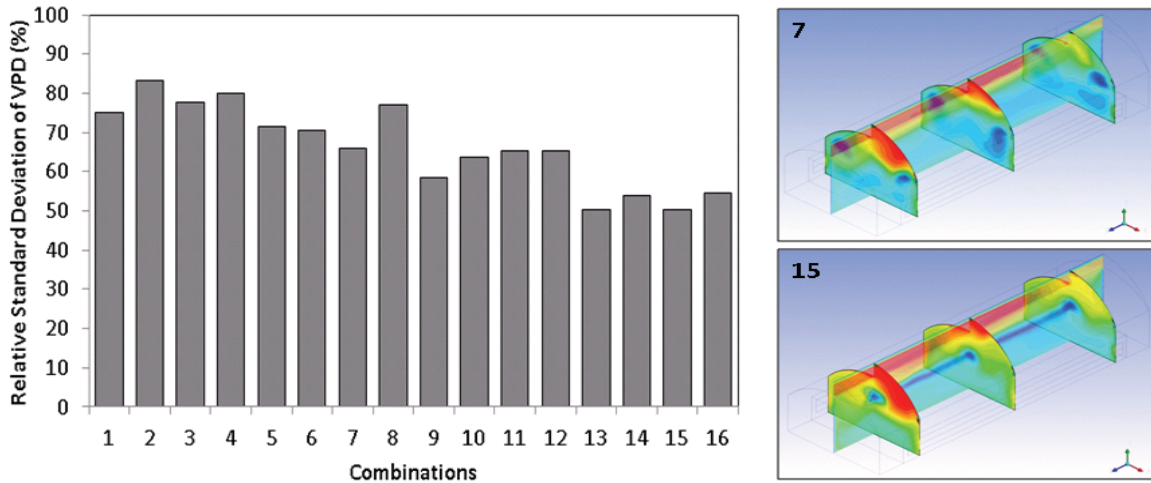


Figure 9. (left) Analysis of climate uniformity using relative standard deviation of VPD distribution and (right) contour diagrams for combinations 7 and 15.

the VPD distribution. The data clearly show that a nozzle placed in the center position and injecting fog in both east and west directions (combinations 9 to 16) produced lower RSD than those observed for combinations 1 to 8. Even more significantly, among the eight combinations tried for the center position nozzle, the 45° nozzle angle (combinations 13 to 16) produced lower RSD than the 0° nozzle angle (combinations 9 to 12).

STATISTICAL ANALYSIS OF FACTORS FOR CLIMATE UNIFORMITY

The validated model was used to generate environmental climate data for 16 theoretical fogging configurations in order to evaluate the effect of four factors on the VPD distribution in the virtual greenhouse interior. Because the model was validated first against the experimental data, the effects of the fogging system could be closely studied at any location of interest. In this study, the region below the gutter was examined because climate uniformity is usually a concern in this region, and for the canopy zone especially. Tomato crops are optimally grown in an environment with a VPD between 0.8 and 1.2 kPa, more preferably at around 1.0 kPa. Therefore, the effects of the various fogging configurations on the VPD average and standard deviation were analyzed.

To evaluate the statistical significance of each factor being considered in the full-factorial design, an ANOVA test, based on the 10,000-point cloud previously discussed, was performed for both the VPD average and the VPD standard deviation. The calculated p-values obtained from the ANOVA model (eq. 14) are shown in table 6:

$$y_{ijkl} = \vartheta + \tau_i + \beta_j + \gamma_k + \alpha_l + \varepsilon_{ijkl} \quad (14)$$

where ϑ is the overall mean response, τ_i is the effect of the side vent opening factor, β_j is the effect of the vertical nozzle position, γ_k is the effect of the nozzle angle, α_l is the effect of the horizontal nozzle position, and ε_{ijkl} is the error term.

A significance level of 0.01 was used to distinguish the significant factors from the non-significant factors.

Although this number is very conservative, differentiating between higher and lower p-values is necessary. Table 6 suggests that the side vent opening is a non-significant effect for VPD average and standard deviation. The vertical nozzle position was also shown to be a non-significant factor for VPD average; however, the vertical nozzle position was shown to be significant for VPD standard deviation. Both nozzle angle and horizontal position were shown to be significant in affecting VPD average and standard deviation. In fact, according to the statistical analysis, horizontal nozzle position was the most significant factor for both VPD average and standard deviation. The results of this statistical analysis are consistent with the analysis that was based on the contour diagrams shown in figures 7 and 8.

CONCLUSIONS

A 3D CFD model was developed and validated in order to predict the environmental variables of a naturally ventilated greenhouse equipped with high-pressure fogging nozzles that were given certain boundary conditions. The model included a porous media component capable of predicting the effect that a mature tomato crop would have on the internal airflow. The model also included a UDF capable of predicting the effects of ET, and an integrated discrete phase modeling component that could predict the effect that the evaporation of fogging droplets would have on the internal greenhouse climate. The validated model was used successfully to evaluate different fogging configurations and thereby determine the changes in greenhouse climate uniformity produced by four factors: side vent opening, vertical nozzle position, nozzle angle, and horizontal nozzle position. The most significant factor for affecting VPD average and standard deviation was shown to be the horizontal nozzle position, while the least significant factor was the side vent opening under the greenhouse design and combinations evaluated in this study.

The information generated by the validated greenhouse

model will enable design engineers to make recommendations for achieving the desired greenhouse climate for a given crop and a greenhouse design. The average VPD values taken from the scenarios involving center and horizontal nozzle configuration were relatively higher than the values taken from the scenarios involving side and horizontal nozzle configuration, and in some cases the values were higher than the desired range, for instance, for a tomato crop, which is more optimally grown in the range of 0.8 to 1.2 kPa, and more preferably at around 1.0 kPa. Based on the contour diagrams, it can be argued that the center-horizontal configuration may produce drier, hotter conditions and should probably be avoided in single-span greenhouses similar to the greenhouse considered in this study. In addition, the diagrams show that positioning the nozzle vertically may not have a significant effect on the VPD values (as confirmed by the statistical analysis). This suggests that greenhouse growers who want to reduce crop wetness could raise their fogging nozzles without significantly affecting climate uniformity. However, the overall effect created may depend on a specific greenhouse design and vent configuration. Thus, using CFD analysis to analyze the effects produced by each vent configuration and fogging arrangement is a good strategy. The contribution of this study is that we present a complex model that is capable of predicting the greenhouse interior climate under the conditions evaluated, as well as methodologies to analyze greenhouse climate uniformity (with RSD analysis of VPD) and the effect of the factors evaluated for a desired climate, in this case based on a desired VPD range.

Our study is meant to serve as an important first step toward achieving a comprehensive model for designing and operating the most efficient greenhouse possible under a given set of climatic conditions. For that purpose, we present several important validation results and also the parameters required to validate the complexity of a given microclimate. In the future, engineers should be able to rely on CFD simulation results during the various stages of greenhouse design. In-depth research is also needed to improve the radiation model to account for different wavelengths and to evaluate the effect of fogging in a time-dependent manner with a transient analysis.

ACKNOWLEDGEMENTS

This research was supported by Research Grant No. IS-4122-08R from the U.S.-Israel Binational Agricultural Research and Development Fund (BARD). UA-CEAC Paper No. D-4342300-04-13.

REFERENCES

ANSYS. 2011. Fluent user manual. Canonsburg, Pa.: ANSYS, Inc. Available at: www.ansys.com.

Bartzanas, T., T. Boulard, and C. Kittas. 2004. Effect of vent arrangement on windward ventilation of a tunnel greenhouse. *Biosystems Eng.* 88(4): 479-490.

Bot, G. P. A. 1983. Greenhouse climate: From physical process to a dynamic model. PhD diss. Wageningen, The Netherlands: Agricultural University of Wageningen.

Boulard, T., and B. Braoui. 1995. Natural ventilation of a greenhouse with continuous roof vents: Measurements and data analysis. *J. Agric. Eng. Res.* 61(1): 27-36.

Boulard, T., and S. Wang. 2002. Experimental and numerical studies on the heterogeneity of crop transpiration in a plastic tunnel. *Comp. and Elec. in Agric.* 34(1-3): 173-190.

Boulard, T., R. Haxaire, M. A. Lamrani, J. C. Roy, and A. Jaffrin. 1999. Characterization and modeling of the air fluxes induced by natural ventilation in a greenhouse. *J. Agric. Eng. Res.* 74(2):195-144.

Bournet, P. E., S. A. Ould Khaoua, and T. Boulard. 2007. Numerical prediction of the effect of vent arrangements on the ventilation and energy transfer in multi-span glasshouse using a bi-band radiation model. *Biosystems Eng.* 98(2): 224-234.

Campan, J. B., and G. P. A. Bot. 2003. Determination of greenhouse-specific aspects of ventilation using three-dimensional computational fluid dynamics. *Biosystems Eng.* 84(1): 69-77.

Choi, C. Y., and S. J. Kim. 1996. Conjugate mixed convection in a channel: Modified five percent deviation rule. *Intl. J. Heat and Mass Transfer* 39(6): 1223-1234.

Dodge, Y., ed. 2003. *The Oxford Dictionary of Statistical Terms*. New York, N.Y.: Oxford University Press.

Fatnassi, H., T. Boulard, and L. Bouriden. 2003. Simulation of climatic conditions in full-scale greenhouse fitted with insect-proof screens. *Agric. and Forest Meteorol.* 118(1-2): 97-111.

Fidaros, D. K., C. A. Baxevanou, T. Bartzanas, and C. Kittas. 2010. Numerical simulation of thermal behavior of a ventilated arc greenhouse during a solar day. *Renewable Energy* 35(7): 1380-1386.

Hong, S.-W., I.-B. Lee, H.-S. Hwang, I.-H. Seo, J. P. Bitog, J.-I. Yoo, K.-S. Kim, S.-H. Lee, K.-W. Kim, and N.-K. Yoon. 2008. Numerical simulation of ventilation efficiencies of naturally ventilated multi-span greenhouses in Korea. *Trans. ASABE* 51(4): 1417-1432.

Kacira, M., T. H. Short, and R. R. Stowell. 1998. A CFD evaluation of naturally ventilated multi-span sawtooth greenhouses. *Trans. ASAE* 41(3): 833-836.

Kacira, M., S. Sase, and L. Okushima. 2004. Optimization of vent configuration by evaluating greenhouse and plant canopy ventilation rates under wind-induced ventilation. *Trans. ASAE* 47(6): 2059-2067.

Kim, K., J. Yoon, H. Kwon, J. Han, J. E. Son, S. Nam, G. Giacomelli, and I. Lee. 2008. 3-D CFD analysis of relative humidity distribution in greenhouse with a fog cooling system and refrigerative dehumidifiers. *Biosystems Eng.* 100(2): 245-255.

Lee, I. B., and T. H. Short. 2000. Two-dimensional numerical simulation of natural ventilation in a multi-span greenhouse. *Trans. ASAE* 43(3): 745-753.

Majdoubi, H., T. Boulard, H. Fatnassi, and L. Bouriden. 2009. Airflow and microclimate patterns in a one-hectare Canary-type greenhouse: An experimental and CFD assisted study. *Agric. and Forest Meteorol.* 149(6-7): 1050-1062.

Mistriotis, A., G. P. A. Bot, P. Picuno, and G. Scarascia-Mugnozza. 1997. Analysis of the efficiency of greenhouse ventilation using computational fluid dynamics. *Agric. and Forest Meteorol.* 85(3-4): 217-228.

Molina-Aiz, F. D., D. L. Valera, and A. J. Alvarez. 2004. Measurement and simulation of climate inside Almeria-type greenhouses using computational fluid dynamics. *Agric. and Forest Meteorol.* 125(1-2): 33-51.

Nebbali, R., J. C. Roy, and T. Boulard. 2012. Dynamic simulation of the distributed radiative and convective climate within a cropped greenhouse. *Renewable Energy* 43: 111-129.

Oke, T. R. 1987. *Boundary Layer Climates*. 2nd ed. New York,

- N.Y.: Taylor and Francis.
- Papadakis, G., M. Mermier, J. F. Meneses, and T. Boulard. 1996. Measurement and analysis of air exchange rates in a greenhouse with continuous roof and side openings. *J. Agric. Eng. Research* 63(3): 219-228.
- Patankar, S. 1980. *Numerical Heat Transfer and Fluid Flow*. New York, N.Y.: Hemisphere Publishing.
- Perdigones, A., J. L. Garcia, A. Romero, A. Rodriguez, L. Luna, C. Raposo, and S. de la Plaza. 2008. Cooling strategies for greenhouses in summer: Control of fogging by pulse width modulation. *Biosystems Eng.* 99(4): 573-586.
- Rohdin, P., and B. Moshfegh. 2007. Numerical predictions of indoor climate in large industrial premises: A comparison between different k - ϵ models supported by field measurement. *Building and Environ.* 42(11): 3872-3882.
- Romero-Gomez, P., I. L. Lopez-Cruz, and C. Y. Choi. 2008. Analysis of greenhouse natural ventilation under the environmental conditions of central Mexico. *Trans. ASABE* 51(5):1753-1761.
- Romero-Gomez, P., C. Y. Choi, and I. L. Lopez-Cruz. 2010. Enhancement of the greenhouse air ventilation rate under climate conditions of central Mexico. *Agrociencia* 44(): 1-15.
- Sapounas, A. A., T. Bartzanas, C. Nikita-Martzopoulou, and C. Kittas. 2008. Aspects of CFD modeling of a fan and pad evaporative cooling system in greenhouses. *Intl. J. Ventilation* 6(4): 379-388.
- Sarlikioti, V., E. Meinen, and L. Marcellis. 2011. Crop reflectance as tool for the online monitoring of LAI and PAR interception in two different greenhouse crops. *Biosystems Eng.* 108(2): 114-120.
- Sase, S., M. Kacira, T. Boulard, and L. Okushima. 2012. Wind tunnel measurement of aerodynamic properties of a tomato canopy. *Trans. ASABE* 55(5): 1921-1927.
- Shklyar, A., and A. Arbel. 2004. Numerical model of the three-dimensional isothermal flow patterns and mass fluxes in a pitched-roof greenhouse. *J. Wind Eng. Ind. Aerodynamics* 92(12): 1039-1059.
- Tadj, N., T. Bartzanas, D. Fidaros, B. Draoui, and C. Kittas. 2010. Influence of heating system on greenhouse microclimate distribution. *Trans. ASABE* 53(1): 225-238.
- Teitel, M., G. Ziskind, O. Liran, V. Dubousky, and R. Letan. 2008. Effect of wind direction on greenhouse ventilation rate, airflow patterns, and temperature distributions. *Biosystems Eng.* 101(3): 351-369.
- Villarreal-Guerrero, F., M. Kacira, E. Fitz-Rodriguez, C. Kubota, G. Giacomelli, R. Linker, and A. Arbel. 2012a. Comparison of three evapotranspiration models for a greenhouse cooling strategy with natural ventilation and variable high-pressure fogging. *Scientia Horticulturae* 134: 210-221.
- Villarreal-Guerrero, F., M. Kacira, E. Fitz-Rodriguez, R. Linker, C. Kubota, G. A. Giacomelli, and A. Arbel. 2012b. Simulated performance of a greenhouse cooling control strategy with natural ventilation and fog cooling. *Biosystems Eng.* 111(2): 217-228.